Photochemical & Photobiological Sciences (2023) 22:147–157
https://doi.org/10.1007/s43630-022-00305-0

ORIGINAL PAPERS

Photochemical defense as trait of fungi from *Cortinarius* subgenus *Dermocybe*

Anna Hannecker[1] · Lesley Huymann[1,2] · Fabian Hammerle[1] · Ursula Peintner[2] · Bianka Siewert[1]

Received: 7 August 2022 / Accepted: 9 September 2022 / Published online: 30 September 2022

Abstract

The photobiological activity of ten colorful species belonging to subgenus *Dermocybe* of the basidiomycete genus *Cortinarius* was investigated. Extracts of all species produced singlet oxygen and are thus photoactive. Pigment analysis was performed and showed similarities of the anthraquinone pigments across the species in dependency to their respective pigmentation types. Detailed content analysis of the pigments in the whole agaricoid fruiting body compared to the three different tissue types (pileus, stipe, and lamellae) revealed that the pigments emodin, dermocybin, and dermorubin, as well as their respective glycosides, are enhanced in the gills. In an independent experiment, the gills were shown to be the most photoactive tissues of the fruiting body. Photobiological experiments with invertebrates (*i.e.*, glassworm *Chaoborus crystallinus*) proved a phototoxic effect of the methanolic extract of the red blood webcap (*Cortinarius sanguineus* var. *aurantiovaginatus*). This work adds further evidence to a common photobiological trait in *Cortinarius* subgenus *Dermocybe* and underpins the possibility of a photochemical defense mechanism in fungi.

Graphical abstract

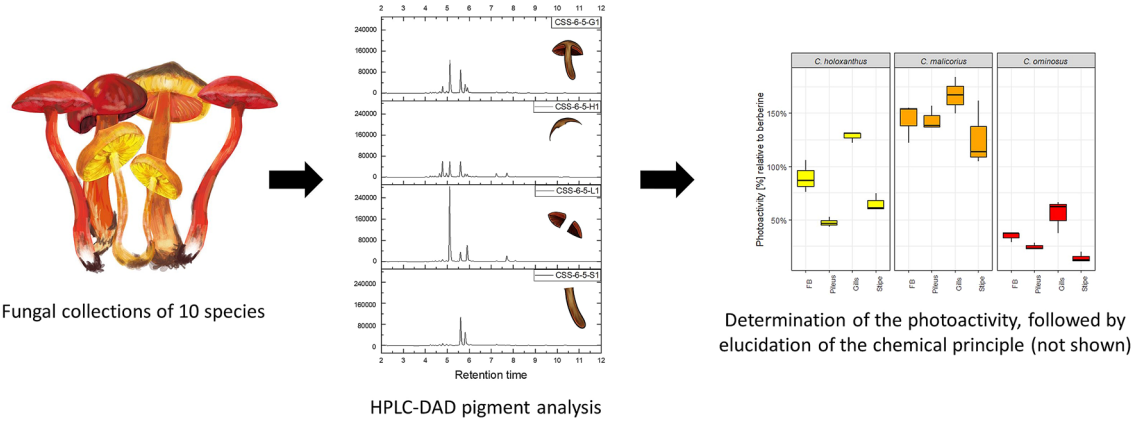

Keywords *Dermocybe* · Fungal photosensitizers · Photochemical defense · Emodin · Anthraquinone · Photoactivity · Phototoxicity

1 Introduction

Hypericin, bergapten, and curcumin belong to the best-known natural photosensitizers [1, 2]. Nonetheless, various other photosensitizers are known to occur in nature, and it can be assumed that many more compounds of this functional class remain to be identified. One overlooked source

✉ Bianka Siewert
bianka.siewert@uibk.ac.at

1 Institute of Pharmacy/Pharmacognosy, Center for Molecular Biosciences Innsbruck, University of Innsbruck, Innrain 80/82, 6020 Innsbruck, Austria

2 Institute of Microbiology, University of Innsbruck, Innsbruck, Austria

for new photosensitizers comprises higher fungi from the division Basidiomycota [3], with more than 30,000 species described to date: recent discoveries highlight pigmented fruiting bodies of certain basidiomycetes as a potent source of photosensitizers [4–6]. Hammerle et al. [6] isolated three new photosensitizers from *Cortinarius uliginosus*. The fungal material was stored for over 40 years, yet the active ingredients —two monomeric and one dimeric anthraquinone— were conserved in the tissue. In detail, the identified photosensitizers were the known fungal anthraquinones dermolutein, dermorubin, and 7,7'-biphyscion [7]. They were characterized by singlet oxygen yields (φ_{Δ}) of 3%, 8%, and 20%, respectively [6].

A photosensitizer per se is a chemical entity capable of transferring absorbed photon energy to its surrounding molecules producing inter alia reactive oxygen species. Typically, a photosensitizer is highly conjugated and thus colored. Next to natural compounds, several synthetic dyes are photosensitizers, such as rose bengal or eosin Y. Activation of photosensitizers via light can induce reactions leading to detrimental biological effects, *e.g.*, lipid peroxidations or oxidative bursts. Therefore, photosensitizers are the active principle of selected therapeutic strategies, such as photoantimicrobial chemotherapy [8] or photodynamic therapy [9–11]. In nature, photosensitizers often play a part in defense mechanisms [2, 3, 12, 13].

Plenty of photosensitizer-producing plants are known compared to fungi, especially basidiomycetes, where only two dermocyboid Cortinarii were studied in detail (i.e., *C. uliginosus* [6] and *C. rubrophyllus* [14]). Nevertheless, photoactivity is not limited to these two species of *Cortinarius*; it was also detected in seven other species belonging to the colorful *Cortinarius* subgenus *Dermocybe* [5, 6]. The ecological function of fungal photosensitizers was explored in collections of *C. rubrophyllus* [15]. Photochemical and analytical studies identified emodin and its monoglucoside as responsible photosensitizers. The content of emodin and also the correlated photoactivity, were highest in the gills. This result hinted toward photochemical defense as one possible ecological function of these pigments.

To test the robustness of this hypothesis, we wanted to investigate whether photoactivity was also enriched in the lamellae of other species. Thus, an extensive analysis of many different species from *Cortinarius* subgenus *Dermocybe* was planned and carried out in 2020. *Cortinarius* subgen. *Dermocybe* represents one moderately supported phylogenomic lineage (BS 93%) within the genus *Cortinarius* [16]. Dermocyboid Cortinarii are characterized by small to medium sized, intensively yellow, orange, red, or olivaceous colored agaricoid fruiting bodies with dry pilei and stipes, and often indistinct or radish-like smell [16–26]. The main objective was to test all species present in one representative habitat type (montane *Picea abies* forests in the Central Alpine area of Tyrol, Austria) to validate photochemical defense strategies in dermocyboid Cortinarii of the northern hemisphere—and fruiting body forming fungi in general—as a trait. In brief, all spotted clusters of dermocyboid Cortinarii with more than five fruiting bodies were collected and submitted to manifold chemical and biological analysis.

Here we present (i) the annotated mycochemical pigment profile of ten different dermocyboid *Cortinarius* species, including five species, which were not mycochemically investigated up to date: *C. hadrocroceus*, *C. holoxanthus*, *C. huronensis*, *C. ominosus*, and *C. fervidus*; (ii) the results of a photochemical screening showing in which parts of the fruiting bodies the phototoxicity is concentrated, and what its chemical origin is, and (iii) the larvicidal effect of the extract from one representative species (*C. sanguineus* var. *aurantiovaginatus*) against Chaoboridae larvae (i.e., *Chaoborus crystallinus*).

2 Results and discussion

2.1 Sampling and ITS-sequencing

The colorful fruiting bodies (FBs) of several dermocyboid Cortinarii were collected in three forest sites in Tyrol (Austria) and identified according to their macroscopic and microscopic characteristics. Due to the wide morphological variety and overlapping morphological characters, a reliable identification beyond species complexes (i.e., species with predominantly yellow, red, and orange lamellae) was not always possible. In consequence, the fungi were initially sorted according to their pigmentation type. The latter was defined by Gruber [27] based on the appearance of the gills and the detected anthraquinones. It was later extended by Keller [28] as well as Høiland [17]. Five types are known, whereof three are relevant for this study (i.e., Cinnamomea, Sanguinea, and Malicoria type, which have yellow, red, and orange gills) and are distinguished by their major pigment/s (see Table S2).

A trustworthy assignment was impeded by the lack of a recent taxonomic key containing all dermocyboid Cortinarii. Thus, after processing and air-drying, DNA extraction was performed, and the internal transcribed spacer (ITS) sequences were analyzed. As a result, many unexpected species were observed: especially the collections of fruiting bodies belonging to the Cinnamomea (yellow) and the Sanguinea (red) pigmentation type [28] showed a great species diversity; the rarely confirmed species *C. holoxanthus*, *C. huronensis*, and *C. hadrocroceus* were, for example, identified. In contrast, the frequently reported, morphologically similar species *C. croceus* and *C. bataillei* were not confirmed, even though macroscopical features and the utilized

identification keys 'Kleine Kryptogamenflora' [29] or Funga Nordica [30] initially hinted toward those species.

Another challenging, morphologically very similar pair of species are *C. malicorius* and *C. rubrophyllus*. On a macroscopic level, they differ in the orange color of the veil remnants on the stipe and the brim of the pileus [30]. However, phylogenetic analysis allowed a precise identification.

Most collections with red pilei and red lamellae, and thus belonging to the Sanguinea pigmentation type, were identified as *C. sanguineus* var. *aurantiovaginatus* (12 of 21) or *C. ominosus* (5 of 21). Nevertheless, also some rare species were discovered like *C. fervidus*, *C. purpureus*, and *C. vitiosus*. The typical habitat of all collected dermocyboid Cortinarii was *Sphagnum* bog co-dwelled with young conifers (e.g., *Picea abies* or *Pinus sylvestris*). Interestingly, several dermocyboid Cortinarii species are often occurring intermixed with each other or intermixed with other species within one square meter. This made the identification of closely related species especially challenging.

2.2 Experimental design

Altogether, 49 collections belonging to ten different dermocyboid *Cortinarius* species (see Table S1) were gathered and processed (i.e., identification, logging, separating into different tissues, and air-drying). This high diversity of different species, especially the rare species, prompted our interest in testing the hypothesis that the photoactivity of dermocyboid Cortinarii is concentrated in their reproductive organs. Thus, we used collections (representing biological replicates) belonging to ten different species (see Figure S1-S10) for our extensive HPLC-DAD(-MS) and photoactivity analysis. At least five fruiting bodies were analyzed of each collection. For *C. hadrocroceus*, *C. malicorius*, *C. ominosus*, and *C. sanguineus* var. *aurantiovaginatus*, even ten fruiting bodies of one collection were examined. All individually collected fruiting bodies were processed prior to air-drying. In detail, the sporocarp was cut lengthwise into two halves, whereby one half was further separated into the pileus, stipe, and gills. This labor-intensive approach was chosen to reduce the effect of abiotic and biotic factors (e.g., temperature or age), which affect the content of the secondary metabolites. If the samples had been pooled, an undesired level of uncertainty would have been gained. Where the biomaterial allowed it, three technical replicates were investigated. In sum, 533 extracts were analyzed and statistically processed.

2.3 Photochemical testing

The extracts of the fruiting bodies and the respective tissues (pileus, stipe, and gills) were submitted to the DMA-assay (9,10-dimethylanthracene, a chemical probe for singlet oxygen [5]) to test whether photoactivity is a common phenomenon in the AQ-producing species of *Cortinarius* subgenus *Dermocybe*. All species produced singlet oxygen, as depicted in Supplementary Figure S11 and Table S3, with a relative photoactivity of at least $33 \pm 15\%$ (for *C. ominosus*) compared to the natural photosensitizer berberine. Extracts of the root of *Berberis ilicifolia* containing berberine [31] yielded a relative photoactivity value of 29% [6]. Evaluating just the complete basidiocarps, extracts from fungi of the Malicoria pigmentation type (*C. malicorius* and *C. rubrophyllus*) were the most active, followed by those from the Sanguinea type and the Cinnamomea type. In the present set of fruiting bodies, no clear ranking between the latter two pigmentation types could be drawn, which seemingly contradicted our previous results [6], where species of the Cinnamomea pigmentation type were found to be highly active (average photoactivity 180–260%). Nevertheless, the species analyzed in this study were different ones (i.e., *C. olivaceofuscus*, *C. uliginosus*, and *C. cinnamomeoluteus vs C. holoxanthus*, *C. huronensis*, and *C. hadrocroceus*) and the extracts were prepared in another manner (i.e., sequential extraction with petroleum ether and methanol vs methanol only). The most prominent difference—and probably the reason behind these diverging results—was, however, the age; the basidiocarps of the initial study [6] were sourced from an herbarium and were up to 45 years old. As a consequence, *e.g.*, the air and light unstable pre-anthraquinones flavomannin-6,6′-di-*O*-methyl ether (FDM) (**11**) and anhydroflavomannin-6,6′-di-*O*-methyl ether (AFDM) (**14**) [32, 33] were nearby completely oxidized to 7,7'-biphyscion (**15**), the most active photosensitizer isolated from *C. uliginosus*. In the present study, however, freshly collected and air-dried fruiting bodies were investigated, thus the precursor FDM (**11**) was still present as major compound. In another recent study, the photoyield of FDM (**11**) was determined to be $\varphi_{\Delta} = 2\%$ [14]. 7,7'-Biphyscion (**15**), in contrast, yields ten times more singlet oxygen ($\varphi_{\Delta} = 20\%$), corroborating this explanation.

Strikingly, independent of the ability to produce singlet oxygen ($^1O_2$), our analysis showed that the extracts of all tested lamellae produce $^1O_2$ the most efficiently (Fig. 1). This also holds true for *C. huronensis* and *C. vitiosus* if one processes the data in such a way that the results of the individual investigated tissues are correlated to the corresponding individual whole half fruiting body, verifying the necessity of our tedious experimental design. A clear tendency was shown for all species, though a significant effect was just calculated for *C. hadrocroceus*, *C. holoxanthus*, and *C. purpureus*. A larger dataset with more individual samples and consequently more data points as part of future research projects will increase the degree of freedom and thus yield true significance. Compared to the fleshy stipes, the filigree nature of gills resulted in extracts of high anthraquinone content [15]. A flaw in the DMA-assay (*i.e.*, the extracts of the

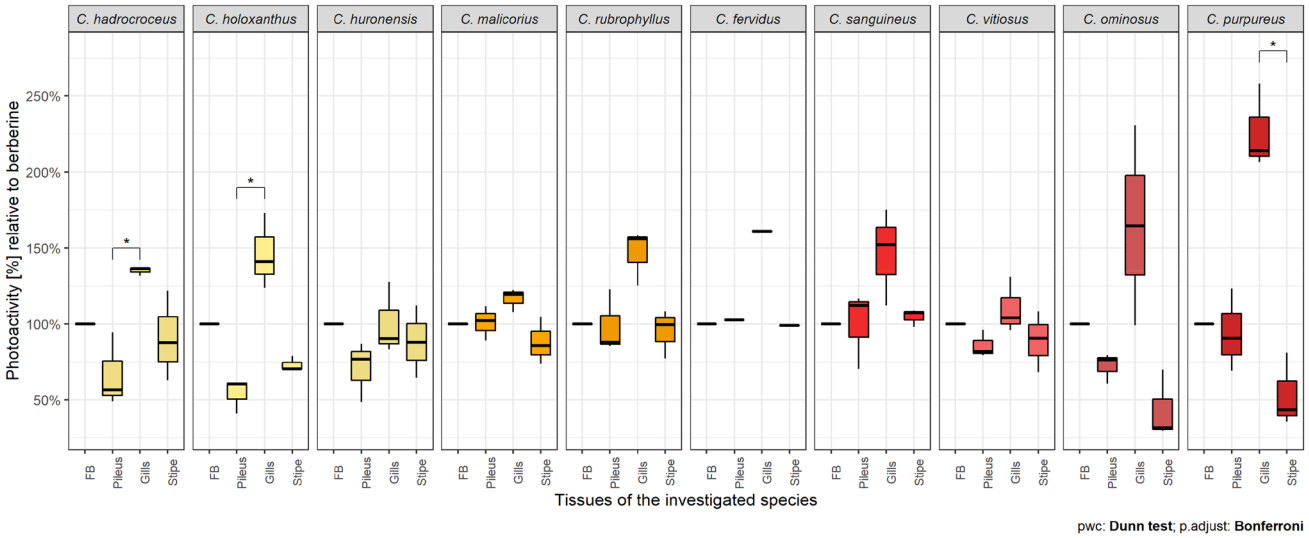

Fig. 1 Distribution of the singlet oxygen generation across the different tissues of all ten investigated species. The results of the individual tissues were normalized to the respective whole half fruiting bodies, to allow easy recognition of the accumulation of photoactivity. Due to the limited sample size of *C. fervidus* only technical replicates were measured

gills yield a false-positive result) is debarred by an included correction factor: the results of the DMA-quenching are corrected by the probability of the absorption; thus, solely a higher concentration of anthraquinones does not lead to a higher $^1O_2$ production value [5].

In short, we reproduced not only the results of *C. rubrophyllus* collected in 2019 [15], showing that the photoactivity is steadily enhanced in the gills, even in collections of different years and sites, but also significantly extended the number of photoactive dermocyboid Cortinarii. In total, the number of *Cortinarius* subgenus *Dermocybe* species investigated for their photoactivity increased to sixteen (*i.e.*, *C. cinnabarinus* [6], *C. cinnamomeoluteus* [6], *C. croceus* [5], *C. hadrocroceus*, *C. holoxanthus* [14], *C. huronensis*, *C. malicorius*, *C. olivaceofuscus* [6], *C. ominosus*, *C. purpureus* [6], *C. fervidus*, *C. rubrophyllus* [14], *C. semisanguineus* [6], *C. sanguineus* var. *aurantiovaginatus*, *C. uliginosus* [6], and *C. vitiosus*). Thus, this result substantiated the strong prospect that photoactivity is a common trait of dermocyboid Cortinarii.

2.4 Mycochemical analysis

HPLC-DAD-MS analysis was conducted of all extracted whole half fruiting bodies. A Synergi Max-RP column was chosen for the analysis, which is excellent for selectively separating different aromatic compounds with a wide range of polarities. Analysis of the MS signals (see Figure S12–19 for selected examples), the UV–Vis absorption, and the comparison with authentic samples (*i.e.*, **1**, **6**, **7**, **8**, **9**, **11**, **12**, **13**, and **15**) allowed the annotation of all major and most minor pigments. As depicted in Fig. 2, up to seventeen different peaks were identified. Generally, they can be classified into glycosides of the monomeric acidic and neutral anthraquinones (**1**–**7**) eluting in the front (r_t = 3–5 min), followed by the acidic monomers (dermolutein (**8**), dermorubin (**9**), as well as endocrocin (**10**)). In the middle (r_t = 6.5 min), the elution of the dimeric pre-anthraquinone FDM (**11**) is observed. In the apolar region (r_t > 7 min), the neutral anthraquinones (emodin (**12**) and dermocybin (**13**)) eluted, followed by the oxidized derivatives of FDM (**11**), *i.e.*, AFDM (**14**) and 7,7′-biphyscion (**15**). Minor pigments as, *e.g.*, dermoglaucin or the chlorinated anthraquinones were not clearly detected in the MS-spectra. Nevertheless, that might be explained by the low concentration and non-optimized MS parameters.

The obtained pigment profiles of ten dermocyboid Cortinarii confirmed the pigment classification according to Keller (1982) (Table S2). Depending on the age and the extraction procedure, the major pigments FDM (**11**) (in the absence of emodin (**12**)), emodin (**12**), and dermocybin (**13**), including the glycosidic derivatives of these monomers, serve well as markers for the yellow (Cinnamomea), orange (Malicoria), and red (Sanguinea) pigmentation type, respectively. In the individual groups of pigmentation types, minor differences can help to differentiate the species (e.g., *C. malicorius* and *C. rubrophyllus* can be distinguished by the variety of acidic anthraquinones (*e.g.*, dermorubin (**9**)). The yellow species seem to differ primarily in the diversity of glycosylated monomeric anthraquinones: while in *C. huronensis,* four different mono- and di-glycosides were annotated (*i.e.*, dermolutein-di-glycoside (**2**), dermocybin-di-glycoside

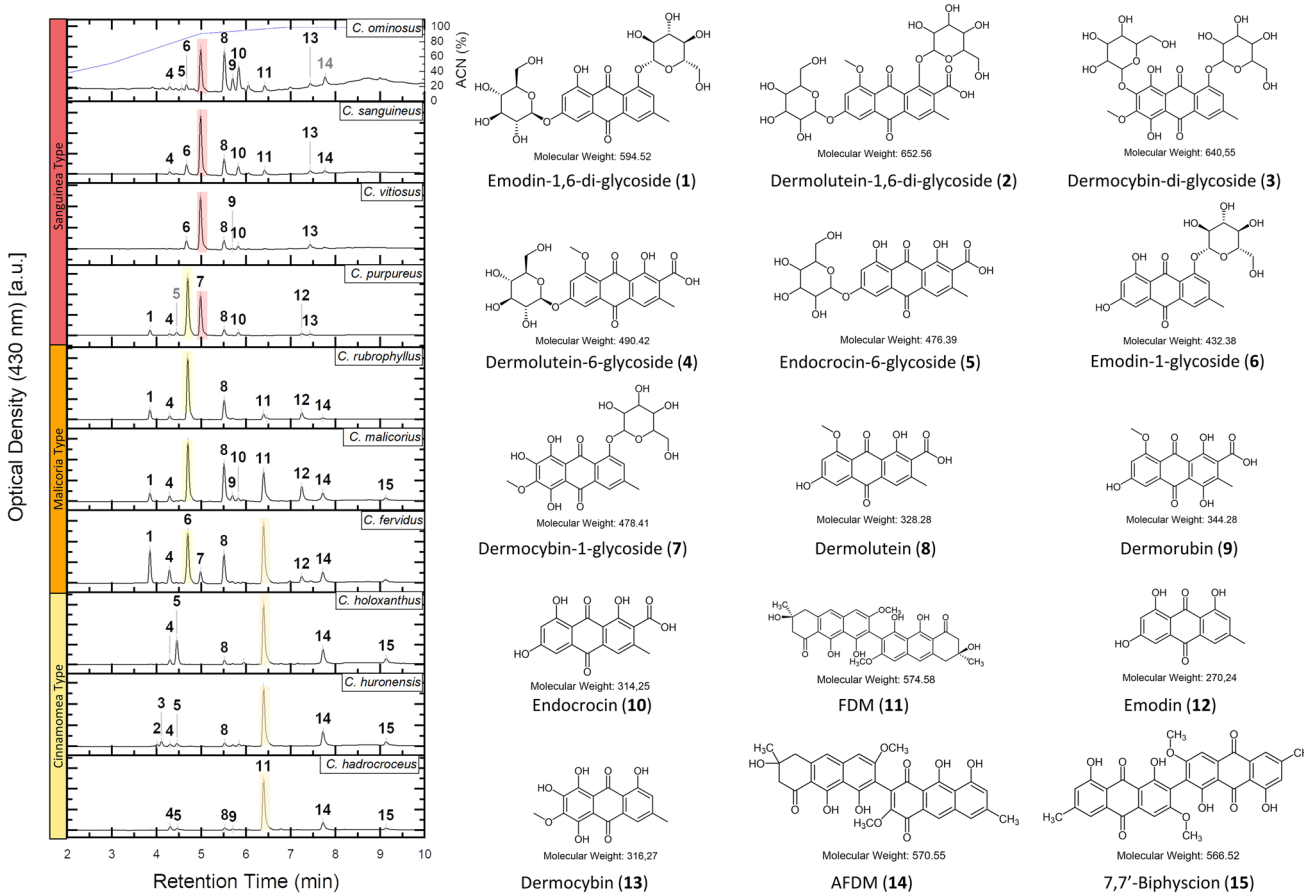

Fig. 2 HPLC–DAD fingerprint analysis of all investigated species with putative annotations of the major and most of the minor pigments. A Synergi Max RP column was used as stationary phase and H_2O/ACN (+0.1% FA) as mobile phase. The gradient is displayed in the upper chromatogram (*Cortinarius ominosus*). The injection volume was 5 µL. Grey expressed numbers in the HPLC diagram indicate uncertainty in the assignment due to low resolution in the respective MS spectrum. Stereochemistry of the glycosides is shown were known from a previous study [14]. For an increased readability, the numbers of the major AQs (**6**, **7**, **11**) were only displayed once and thereafter highlighted in color (yellow … emodin-1-glycoside (**6**), red … dermocybin-1-glycoside (**7**), and orange … FDM (**11**))

(**3**), dermolutein-glycoside (**4**), and endocrocin-glycoside (**5**)), in *C. holoxanthus* and *C. hadrocroceus* only **4** and **5** were detected. The latter two species were distinguishable by the content of **4** and **5**. Nevertheless, further studies are needed to verify these annotated AQ-glycosides' chemical nature and validate if this is a robust differentiator.

Analysis of *C. fervidus*, being represented by a collection comprising only four fruiting bodies, led to the identification of all three major pigments (*i.e.*, **6**, **8**, **11**). Thus, its pigmentation type could be described as a blend of three different types. A detailed phylogenetic and mycochemical investigation is part of future projects.

The chromatograms of the red species, dominated by dermocybin-glycoside (**7**), can only be distinguished by their minor compounds. In our dataset, identification based on the pigment fingerprint is possible. Nevertheless, verification is needed to confirm HPLC-DAD analysis as a suitable tool for chemotaxonomy, which is urgently required to complement phylogenetic analyses with low resolution, as typical for this group of fungi. Larger datasets of unambiguously identified fruiting bodies are therefore required. Such datasets should contain different basidiocarps from different locations, collected under various abiotic conditions and at different stages of development. Furthermore, the dataset should comprise fruiting bodies of all known dermocyboid Cortinarii, *i.e.*, also including species described from the Southern Hemisphere. All mycochemical well-described species should be included to train an algorithm with as many data points as possible. With such a dataset in hand and the means of modern data processing (*i.e.*, machine learning), a mycochemistry-aided identification will be possible.

This report presents—to the authors' best knowledge—for all included fungi, the first mycochemical pigment profile based on combined chromatographic and mass-spectrometric means. Chromatographic investigations are known for

C. holoxanthus [28], *C. malicorius* [28], *C. purpureus* [28], *C. sanguineus* [28, 34], and *C. vitiosus* [34]. They coincided with the results presented here.

2.5 Identification of the active principle

After the assignment of all relevant peaks, we analyzed which pigments were significantly more enhanced in the lamellae as compared to the other parts of the fruiting body. Data processing was done in such a way that the individual components were always correlated to their content in the respective whole half fruiting body (to account for concentration differences due to age or other abiotic factors across the collection). Furthermore, the probability of photon absorption ($\lambda = 468$ nm) was included by expressing the fraction of that peak in the total extract. As depicted representatively in Fig. 3, and as a complete set in the ESI (Figure S20–27), for each species, we were able to putatively assign one or two pigments as responsible for the high phototoxicity of the gills.

The putatively responsible compounds seem to be the same for each pigmentation type (refer to supplementary

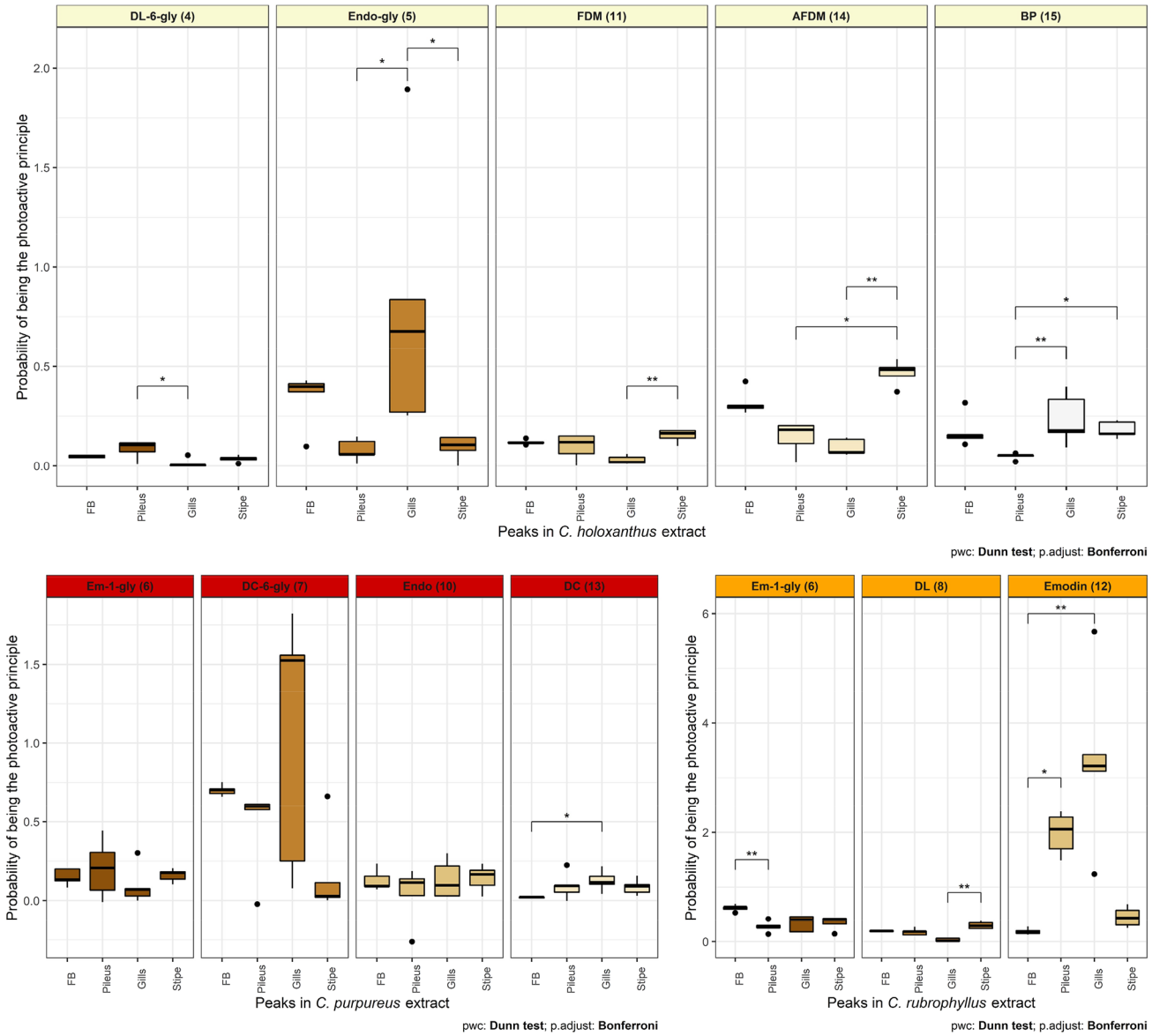

Fig. 3 Distribution of the respective major components in the different tissues of fungal fruiting bodies. Represented is the portion of the individual pigment accounting for the total absorbance at 468 nm. For *C. holoxanthus* and *C. purpureus* only those fungi tested in the DMA assay were used to allow a direct comparison. *FB* fruiting body; DL-6-gly Dermolutein-6-glycoside; *Endo-gly* endocrocin-glycoside; *Em-1-gly* emodin-glycoside, *DC-6-gly* Dermocybin-6-glycoside

part Figure S20–28). For the Malicoria type, emodin (**12**) was identified as significantly higher expressed in the gills, which reproduced our data from fungi collected in 2019 [15], where we investigated over twenty individual fruiting bodies of *C. rubrophyllus*. For *C. holoxanthus, C. huronensis*, *C. hadrocroceus*, and thus for all studied Cinnamomea type fungi, peak **5** —putatively assigned as the glycoside of endrocrocin (**5**)—was shown to be enhanced in the gills. Furthermore, **15** was proven to be enriched in the gills of *C. huronensis* and *C. holoxanthus*, which correlates with the high photoactivity, as **15** is described by a photoyield of 20%. Neither the glycoside of endocrocin (**5**) nor endocrocin (**10**) itself was yet photochemically characterized; thus, a precise photochemical statement is not possible. Nevertheless, from emodin and its glycosides, it is known that the photoactivity is retained, even if it is reduced [14]. For the species belonging to the Sanguinea type, dermocybin (**13**) and its glycoside (**7**), as well as emodin (**12**) (Figure S21, S23), seem to be responsible. Nevertheless, more detailed investigations are needed due to the complexity of the Sanguinea-type extracts (especially of the minor compounds) and the wide range in the contents of investigated pigments.

In sum, the detailed HPLC-DAD analysis of individual fruiting bodies of ten different dermocyboid Cortinarii showed that (i) the photoactivity is concentrated in the gills and that (ii) monomeric AQs, as well as their glycosides, are responsible for this action. That the gills contain the highest content of a toxin is a phenomenon well known in the genus *Amanita*. For *Amanita phalloides* [35, 36], *A. exitialis* [37], and *A. fuliginea* [38] it was shown that alpha-amanitin is concentrated in the gills followed by the cap. Thus, our results fit into the general body of knowledge.

2.6 Photolarvicidal activity

To test for biological function, i.e., photochemical defense, a photoinsecticidal assay utilizing Chaoboridae larvae (*Chaoborus crystallinus*) was performed according to Preuß and colleagues [39]. In brief, ten larvae were treated with a methanolic extract of *C. sanguineus* var. *aurantiovaginatus,* one of the most abundant dermocyboid *Cortinarius* species in Tyrol, for 1 h. After incubation, one set of larvae was exposed to blue light ($\lambda = 468 \pm 27$ nm, $H = 74.16$ J/cm^2, $t = 60$ min) while the second set was stored in the dark, to evaluate the dark toxicity of the extract. The dead larvae were counted after three hours. As depicted in Fig. 4a, the irradiation alone—without extract—showed no effect. The treatment with the extract of *C. sanguineus* var. *aurantiovaginatus* induced a dose-dependent lethal effect in the dark as well as under blue light illumination. The irradiated population, however, was significantly more affected than the respective dark population.

The transparency of the larvae allowed us furthermore to observe the accumulation of the colored anthraquinones (Fig. 4b). In the dark, the anthraquinone fraction accumulated in the intestine of the larvae (Fig. 4b, middle). Sunlight irradiation induced a lethal effect. Microscopic investigation showed that the larva was affected, and an extensive staining of the entire body was observed. In conclusion, the outcome of this experiment supports our hypothesis of photoactivated defense as a common trait of dermocyboid Cortinarii.

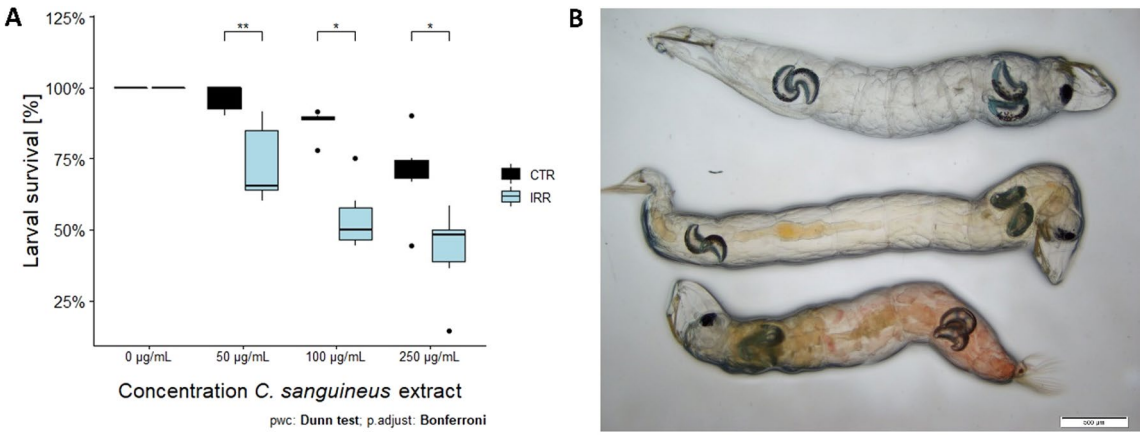

Fig. 4 **A** Larval phototoxicity of a *Cortinarius sanguineus* var. *aurantiovaginatus* extract tested at different concentrations and under blue light irradiation (IRR, $\lambda = 468 \pm 27$ nm, $H = 74.16$ J/cm^2, $t = 60$ min) or in the dark (CTR). The obtained data were not normally distributed. Thus, a Kruskal–Wallis test was performed with the following significance levels: $^*p < 0.05$, $^{**}p < 0.005$. **B** Micrographs of untreated (upper), dark treated (250 µg/mL, dark, middle), and light treated (250 µg/mL, sunlight, lower) *Chaoborus crystallinus* larvae

3 Conclusion

Taking together, we could prove that each of the ten species of *Cortinarius* subgenus *Dermocybe* was (i) photoactive and (ii) that at least one anthraquinone was enhanced in the gills. The anthraquinones being putatively responsible for the photoactivity correlated well with the glycoside(s) of the most abundant monomeric anthraquinone, or the monomeric anthraquinone itself (*i.e.*, emodin (**12**) for the Malicoria type and probably dermocybin (**13**) and **12** as well as their glycosides **3** and **7** for the Sanguinea type). Furthermore, we could show that the pigment extract is phototoxic for larvae. Thus, we conclude that photoactivity is a typical trait of *Cortinarius* subgenus *Dermocybe* and is most likely part of a photochemical defense mechanism. How these pigments and the photochemical defense mechanism evolved and which role the ectomycorrhizal partners of these fungi play are parts of future research.

4 Materials and methods

4.1 Chemicals and reagents

Solvents were purchased from VWR (VWR International, Vienna, Austria). Acetone was distilled prior to use. The HPLC experiments were performed with solvents from Merck (Merck KGaA, Darmstadt, Germany) having pro analysis (p.a.) quality. 9,10-Dimethylanthracene (product number: D0252) was purchased from TCI Deutschland GmbH (Eschborn, Germany). Ultrapure water was generated using the Sartorius arium® 611 UV purification system (Sartorius AG, Göttingen, Germany).

4.2 Instrumentation

The Sartorius Cubis®-series balance (Sartorius AG, Göttingen, Germany) was utilized as well as the ultrasonic baths Sonorex RK 52 and Sonorex RK 106 (BANDELIN electronic GmbH & Co. KG, Berlin, Germany). Mixing was performed with the vortex mixer Vortex-Genie 2 (Scientific Industries, Inc., Bohemia, New York). Centrifugation was done with the Eppendorf centrifuge 5804 R (Eppendorf AG, Germany). Adjustment of pH-values was conducted with the pH-meter Mettler Toledo SevenMulti (Mettler-Toledo GmbH, Vienna, Austria). The experimental setup for the DMA-assay and the photocytotoxic study comprised a LED-panel ($\lambda = 468$ nm (1.24 J cm^{-2} min^{-1})), which was built at University Leiden (published in Hopkins et al. [40], characterization of the one used specifically [5]), and the power adaptor Agilent E3611A DC Power Supply (Agilent Technologies, Inc., Santa Clara, United States). Optical densities were measured with the plate reader Tecan Spark® 10 M (Tecan Group Ltd., Männedorf, Switzerland). HPLC-DAD-ESI-MS analysis was carried out with the modular system Agilent Technologies 1260 Infinity II equipped with a quaternary pump, vial sampler, column thermostat, diode-array detector, and an ion trap mass spectrometer (amaZon, Bruker, Bremen, Germany). Moreover, the HPLC-system SHIMADZU HPLC/UPLC-UFLC XR, with binary pump, vial sampler, column thermostat, and diode-array detector was used (SHIMADZU CORPORATION, Kyoto, Japan).

4.3 Mushroom collection and preparation

Cortinarius spp. fruiting bodies were collected in Tyrol (Austria) from July to October 2020. The authors names, reference voucher numbers, collection dates, information concerning sampling sites, soil and habitat information, as well as the photographic documentation are given in the supplementary (Table S1 and Figure S1–S11). The identification of the fungi was based on macroscopic and microscopic morphological characters, habitat characters, as well as on comparative rDNA ITS sequence analysis. For morphology-based confirmation of identity, the taxonomic keys from Moser [29] and Knudsen and Vesterholt [30] were utilized. Voucher specimens were deposited in the mycological collection of the Natural Sciences Collections of the Tiroler Landesmuseen (Natural Sciences Collections of the Tiroler Landesmuseen (IBF), Krajnc-Straße 1, 6060 Hall, Austria, http://www.tiroler-landesmuseen.at). Prior to the drying process, the fruiting bodies were cleaned. Briefly, they were scrubbed with a brush and carefully divided into two sagittal pieces. One sagittal part was further divided into pileus, gills, and stipe. After separation, the fungal biomaterial was dried at room temperature in the shade and stored in small paper bags.

4.4 DNA-extraction and rDNA ITS sequencing

The DNA-extraction and barcode sequencing was done as previously reported [15]. Methodological details are provided in the supplementary (see supplementary information, Sect. 1.3).

5 HPLC analysis of fungal extracts

5.1 Extract preparation

The dried fruiting body halves and fungal tissues (i.e., pileus, gills, and stipe) were ground with mortar and pestle. Ultrasonic extraction of the powdered biomaterials was performed under exclusion of sunlight at room temperature

($T = 22$ °C). In detail, the ground samples ($m = 10$–28 mg) were extracted ($t = 10$ min sonification) with methanol ($V = 1.5$ mL), centrifuged, and the solution decanted. This extraction process was performed five times in total and the supernatants were combined. The extracts were dried in the dark under an air stream and kept in a freezer ($T = -20$ °C) before use. Extraction yields ranged, e.g. from 0.1 to 14.2 mg or 20–56% w/w for *C. hadrocroceus*.

5.2 HPLC-method

All extracts were analyzed by HPLC using a Synergi MAX-RP 80 Å column (150 × 4.60 mm, 4 micron) from Phenomenex (Aschaffenburg, Germany) as stationary phase. The mobile phase (A) was water, (B) consisted of acetonitrile and 0.1% formic acid. Elution was performed in gradient mode starting with 10% B to 50% B from $t = 0$–3 min, 50% B to 90% B from $t = 3$–5 min, 90% B to 99% B from $t = 5$–7 min, 99% B to 10% B from $t = 7$–11 min, followed by 4 min of re-equilibration with 90% A. The DAD was set to $\lambda = 430$ and 478 nm, and flow rate, sample volume, and column temperature were adjusted to $Q = 1.0$ mL/min, $V = 5$ µL, and $T = 40$ °C, respectively.

5.3 HPLC analysis of extracts

The extracts were solved in DMSO, and the volume was calculated such that the methanolic extract resulting from $m = 25.0$ mg of starting material was solved in $V = 1$ mL stock solution.

5.4 Statistical analysis

Peak quantification was performed automatically by Origin 2020 and manually checked for each extract so that the baseline always fitted. The obtained peak areas were processed in Excel 365 and using R Statistical Software (v4.1.2; R Core Team 2021) [41]. The packages tidyverse, dplyr, ggpubr, and rstatix were utilized.

For each relevant dataset, a Shapiro–Wilk test was performed. For all analyzed data sets normal distribution was not given, thus a Kruskal–Wallis test was performed with the Dunn-test to account for the multiple comparison and Bonferroni *p* adjustment. The variable "Probability of being the photoactive principle" was calculated as product of the relative peak area of the peak in the individual tissues as compared to the fruiting bodies and the fraction of that peak area divided by the sum of all analyzed peaks in that tissue absorbing at $\lambda = 468$ nm. See Figure S29 for the processing workflow.

5.5 DMA-assay

The assay was performed—with slight modifications—as published previously [5]. In short, the extracts solved in a DMSO stock (1 mg/mL) were diluted with an ethanol or DMA solution and transferred to a 96 well plate. DMSO ($V = 10$ µL) was used as negative control and berberine ($c = 1$ mg/mL, $c = 2.97$ mM, DMSO, $V = 10$ µL) as positive control [42]. Thereafter, optical densities (OD) at specific wavelengths (i.e., $\lambda = 377$ and $\lambda = 468$ nm) were measured with a plate reader, followed by four cycles of blue light irradiation ($\lambda = 468$ nm, 1.24 J cm^{-2} min^{-1}, $t = 5$ min) and OD measurements. The measurements were done as technical duplicates. The results of the DMA-assay were displayed as the mean ± standard error. A Kruskal–Wallis test followed by the Dunn-test and Bonferroni *p* adjustment were used to statistically evaluate differences between the relative singlet oxygen production values.

5.6 Determination of photolarvicidal activity

Fresh *Chaoborus crystallinus* larvae were sourced from the local pet store (Kölle Zoo, Innsbruck). Ten larvae were transferred to each well of a 12-well plate, the original liquid was aspirated and replaced by larvae buffer (5% w/w glucose in phosphate buffered saline (PBS)) loaded with different concentrations of the methanol extract of *C. sanguineus* var. *aurantiovaginatus* ($V = 2$ mL). First, the extract was dissolved in H_2O/EtOH (9:1 v/v) and further diluted with the puffer to obtain the following final concentrations: $c = 0$, 50, 100, and 250 µg/mL. After 1 h of incubation, irradiation ($\lambda = 468 \pm 27$ nm, $H = 74.16$ J/cm^2, $t = 60$ min) was performed with the LED-setup characterized in Siewert et al. [5]. After additional 3 h of incubation in the dark, dead larvae were defined by either a milky white appearance or by unresponsive behavior to being punctured by a needle. The survival rate was calculated of six biological replicates of 10 individual larvae. The data were processed with Excel 365 and R. The packages tidyverse, dplyr, ggpubr, and rstatix were utilized. For each relevant dataset, a Shapiro–Wilk test was performed. As the groups were not normally distributed, the level of significance was tested via a Kruskal–Wallis test followed by Dunn-test to account for the multiple comparison and a Bonferroni *p* adjustment.

Supplementary Information The online version contains supplementary material available at https://doi.org/10.1007/s43630-022-00305-0.

Author contributions Conceptualization—BS and UP; collection and processing of the fruiting bodies—LH; DNA extraction and ITS-analysis—LH and UP; extract preparation and chemical analysis—AH; DMA analysis—AH and FH; data treatment and statistically analysis—BS and AH; insecticidal assay—FH; manuscript draft—BS;

writing—review and editing, AH, LH, FH, UP, and BS; visualization—BS; project administration—BS; funding acquisition—BS.

Funding Open access funding provided by University of Innsbruck and Medical University of Innsbruck. The Tyrolian Science fund is acknowledged for the funding of the irradiation setup and the collection. P. Vrabl and H. Stuppner are thanked for their valuable input and the discussions.

Availability of data and material The ITS sequences of all studied fungi are deposited at the GenDatabank. Please refer to the supplementary part for a detailed table containing all needed numbers. Voucher material of all studied species is deposited at the Tiroler Landesmuseum (IBF) in Hall (Austria).

Declarations

Conflict of interest The authors declare no competing interest.

References

1. Siewert, B., & Stuppner, H. (2019). The photoactivity of natural products—An overlooked potential of phytomedicines? *Phytomedicine, 60*, 152985.
2. Flors, C., & Nonell, S. (2006). Light and singlet oxygen in plant defense against pathogens: Phototoxic phenalenone phytoalexins. *Accounts of Chemical Research, 39*(5), 293–300.
3. Siewert, B. (2021). Does the chemistry of fungal pigments demand the existence of photoactivated defense strategies in basidiomycetes? *Photochemical and Photobiological Sciences, 20*, 475–488.
4. Fiala, J., et al. (2021). A new high-throughput-screening-assay for photoantimicrobials based on EUCAST revealed photoantimicrobials in Cortinariaceae. *Frontiers in Microbiology, 12*, 703544.
5. Siewert, B., et al. (2019). A convenient workflow to spot photosensitizers revealed photo-activity in basidiomycetes. *RSC Advances, 9*(8), 4545–4552.
6. Hammerle, F., et al. (2022). Targeted isolation of photoactive pigments from mushrooms yielded a highly potent new photosensitizer: 7,7′-biphyscion. *Scientific Reports, 12*(1), 1108.
7. Steglich, W., et al. (1972). Isolation of flavomannin-6,6′-dimethyl ether and one of its racemates from higher fungi. *Phytochemistry, 11*(11), 3299–3304.
8. Wainwright, M., et al. (2017). Photoantimicrobials—Are we afraid of the light? *The Lancet Infectious Diseases, 17*(2), e49–e55.
9. Kessel, D. (2020). Photodynamic therapy: Apoptosis, paraptosis and beyond. *Apoptosis, 25*(9), 611–615.
10. Hamblin, M. R. (2020). Photodynamic therapy for cancer: What's past is prologue. *Photochemistry and Photobiology, 96*(3), 506–516.
11. Vickerman, B. M., et al. (2021). Taking phototherapeutics from concept to clinical launch. *Nature Reviews Chemistry, 5*(11), 816–834.
12. Wainwright, M. (2007). Natural product photoantimicrobials. *Current Bioactive Compounds, 3*(4), 252–261.
13. Berenbaum, M. (1995). Phototoxicity of plant secondary metabolites: Insect and mammalian perspectives. *Archives of Insect Biochemistry and Physiology, 29*(2), 119–134.
14. Hammerle, F., et al. (2022). Optimized isolation of 7,7′-biphyscion starting from Cortinarius rubrophyllus, a chemically unexplored fungal species rich in photosensitizers. *Photochemical & Photobiological Sciences, 21*(2), 221–234.
15. Siewert, B., et al. (2022). The photosensitizer emodin is concentrated in the gills of the fungus *Cortinarius rubrophyllus*. *Journal of Photochemistry and Photobiology B: Biology, 228*, 112390.
16. Liimatainen, K., et al. (2022). Taming the beast: A revised classification of Cortinariaceae based on genomic data. *Fungal Diversity, 112*(1), 89–170.
17. Høiland, K. (1983). Cortinarius subgenus Dermocybe. *Opera Botanica, 71*, 1–113.
18. Kidd, C. B. M., et al. (1985). Thin-layer chromatography as an aid for identification of Dermocybe species of Cortinarius. *Transactions of the British Mycological Society, 85*(2), 213–221.
19. Liu, Y. J., Rogers, S. O., & Ammirati, J. F. (1997). Phylogenetic relationships in Dermocybe and related Cortinarius taxa based on nuclear ribosomal DNA internal transcribed spacers. *Canadian Journal of Botany-Revue Canadienne De Botanique, 75*(4), 519–532.
20. Stefani, F. O., Jones, R. H., & May, T. W. (2014). Concordance of seven gene genealogies compared to phenotypic data reveals multiple cryptic species in Australian dermocyboid Cortinarius (Agaricales). *Molecular Phylogenetics and Evolution, 71*, 249–260.
21. Moser, M. (1972). Die Gattung Dermocybe (Fr.) Wuensche (Die Hautkoepfe). *Schweizerische Zeitschrift fuer Pilzkunde, 50*, 153–167.
22. Moser, M. (1974). Die Gattung Dermocybe (Fr) Wünsche, (Die Hautköpfe). *Schw. Zeitschrift für Pilzkunde., 52*, 9. Sondernummer 92, 129–142.
23. Keller, G., et al. (1988). Chemotaxonomic investigations of species of Dermocybe (Fr.) Wünsche (Agaricales) from New Zealand, Papua New Guinea and Argentina. *Sydowia, 40*, 168–187.
24. Moser, M., & Horak, E. (1975). Cortinarius Fr. und nahe verwandte Gattungen in Südamerika. *Beihefte zur Nova Hedwigia, 52* (Vaduz: J. Cramer. vi, 628, 116, [10] leaves of plates).
25. Soop, K. (2021). *Cortinarius in Sweden* (17th revised ed). Mora.
26. Niskanen, T., et al. (2013). Cortinarius section Sanguinei in North America. *Mycologia, 105*(2), 344–356.
27. Gruber, I. (1970). Anthrachinonfarbstoffe in der Gattung Dermocybe und Versuch ihrer Auswertung fuer die Systematik. *Zeitschrift für Pilzkunde, 36*(1/2), 95–112.
28. Keller, G. (1982). *Pigmentationsuntersuchungen bei europäischen Arten aus der Gattung Dermocybe (FR.) WÜNSCHE* (pp. 110–126).
29. Moser, M. (1983). In H. Gams (Ed.) *Kleine Kryptogamenflora: 2, Pilze, T. b, Basidiomyceten, T. 2: Die Röhrlinge und Blätterpilze: (Polyporales, Boletales, Agaricales, Russulales)/von Meinhard Moser*, 5, bearb. Aufl. ed. Vol. Bd (pp. 1–532). 2b/2. Stuttgart [u.a.]: G. Fischer.
30. Knudsen, H., & Vesterholt, J. (2021). *Funga Nordica: Agaricoid, boletoid and cyphelloid genera*. Copenhagen: Nordsvamp.
31. Ali Redha, A., Siddiqui, S. A., & Ibrahim, S. A. (2021). Advanced extraction techniques for Berberis species phytochemicals: A

review. *International Journal of Food Science and Technology, 56*(11), 5485–5496.
32. Gill, M., & Steglich, W. (1987). *Fortschritte der Chemie organischer Naturstoffe/Progress in the chemistry of organic natural products*.
33. Steglich, W., et al. (1972). Chemotaxonomic studies on mushrooms XX. Pigments of Fungi. VIII. Isolation of flavomannin-6,6'-dimethyl ether and one of its racemates from higher fungi. *Phytochemistry, 11*(11), 3299–304.
34. Räisänen, R. (2019). Fungal colorants in applications—Focus on Cortinarius species. *Coloration Technology, 135*(1), 22–31.
35. Enjalbert, F., et al. (1999). Distribution of the amatoxins and phallotoxins in Amanita phalloides. Influence of the tissues and the collection site. *Comptes Rendus de l'Académie des Sciences-Series III-Sciences de la Vie, 322*(10), 855–862.
36. Kaya, E., et al. (2013). Amatoxin and phallotoxin concentration in Amanita phalloides spores and tissues. *Toxicology and Industrial Health, 31*(12), 1172–1177.
37. Hu, J., et al. (2012). Determination of amatoxins in different tissues and development stages of Amanita exitialis. *Journal of the Science of Food and Agriculture, 92*(13), 2664–2667.
38. Zhou, Q., et al. (2017). Amatoxin and phallotoxin concentrations in *Amanita fuliginea*: Influence of tissues, developmental stages and collection sites. *Mycoscience, 58*(4), 267–273.
39. Preuß, A., Pfitzner, M., & Röder, B. (2019). Mosquito larvae control by photodynamic inactivation of their intestinal flora—A proof of principal study on *Chaoborus* sp. *Photochemical and Photobiological Sciences, 18*(10), 2374–2380.
40. Hopkins, S. L., et al. (2016). An in vitro cell irradiation protocol for testing photopharmaceuticals and the effect of blue, green, and red light on human cancer cell lines. *Photochemical and Photobiological Sciences, 15*(5), 644–653.
41. Team RC. (2021). *R: A language and environment for statistical computing*. Vienna, Austria: R Foundation for Statistical Computing.
42. Oliveira, P. M., et al. (2020). Effect of berberine associated with photodynamic therapy in cell lines. *Photodiagnosis and Photodynamic Therapy, 32*, 102045.